The Novel Tubulin-binding Drug BTO-956 Inhibits R3230Ac Mammary Carcinoma Growth and Angiogenesis in Fischer 344 Rats[1]

Siqing Shan, A. Craig Lockhart, Wilfred Y. Saito, A. Merrill Knapp, Keith R. Laderoute, and Mark W. Dewhirst[2]

Department of Radiation Oncology, Duke University Medical Center, Durham, North Carolina 27710 [S. S., A. C. L., W. Y. S., M. W. D.], and Pharmaceutical Discovery Division, SRI International, Menlo Park, California 94025 [A. M. K., K. R. L.]

ABSTRACT

BTO-956 [methyl-3,5-diiodo-4-(4′-methoxyphenoxy)-benzoate], a novel tubulin-binding drug and thyroid hormone analogue, was originally found to inhibit human carcinoma cell proliferation *in vitro* and to have potent growth delay activity in human breast and ovarian carcinoma xenografts in nude mice. Here we report that BTO-956 given to Fischer 344 rats also inhibits corneal angiogenesis and the growth and neovascularization of the R3230Ac rat mammary carcinoma tumor implanted in skin-fold window chambers. Hydron pellets containing recombinant human basic fibroblast growth factor (50 ng) and Sucralfate (20 μg) were implanted into surgically created corneal micropockets (day 0). BTO-956 was administrated by oral gavage (500 mg/kg, twice a day for 6 days) on days 1–6 (controls received vehicle alone). On day 7, rats received retrogade infusions of India ink via the thoracic aorta to visualize the corneal vasculature. Digitized images of slide-mounted corneas from control and treated animals were taken with a microscope. For the tumor growth and angiogenesis study, small pieces of R3230Ac tumor from a donor rat were implanted into surgically prepared window chambers (day 0). BTO-956 was given during days 5–11, and images of the tumors and their vasculature were recorded on day 12. No body weight loss was observed in either study. BTO-956 significantly inhibited corneal angiogenesis (by 50–80%), as assessed by measurements of limbal circumference displaying neovascularization, vessel length, vascularized area, and vascular area density. In the window chamber assay, tumors from treated animals were >50% smaller than tumors in control animals. In addition, vascular length densities in peripheral tumor zones were 30% less in treated compared with control animals. Together, these findings demonstrate that BTO-956 can inhibit angiogenesis induced by a growth factor in the rat cornea and in the peripheral area of implanted tumors, where tumor angiogenesis is most active.

INTRODUCTION

Angiogenesis, the formation of new vessels from existing vasculature, has a critical role in primary tumor growth, invasion, and metastasis (1). Tumor-associated angiogenesis is a multistep process that is controlled by both positive and negative factors as well as by complex interactions among tumor cells, host endothelium, stromal cells, and extracellular matrix components. Moreover, because tumor vascular networks are formed within microenvironments intrinsic to the tumor mass, they have markedly different properties compared with those in normal tissues. These tissue-level differences make angiogenic tumor endothelial cells an attractive target for the development of new anticancer therapies. Current antivascular or antiangiogenic approaches include treatment with cytotoxic agents having some selectivity for proliferating vascular endothelial cells, natural angiogenesis inhibitors, modified soluble receptors that interfere with angiogenic signal transduction, and synthetic compounds capable of selectively inhibiting endothelial cell proliferation or remodeling of the extracellular matrix (2, 3).

Some conventional anticancer drugs have antivascular or antiangiogenic activity in addition to their cytotoxic effects toward tumor cells (4, 5). For example, tubulin-binding agents that cause mitotic arrest can have antivascular or antiangiogenic activity. Colchicine is a tubulin-binding agent that was reported to produce hemorrhagic necrosis in experimental tumors (6). In addition, colchicine was reported to be cytotoxic toward endothelial cells in capillary sprouts (7). Combretastatin A4, another tubulin-binding molecule isolated from the South African tree *Combretum caffrum*, displays potent and selective toxicity toward tumor vasculature and to perturb tumor perfusion and energy status (8, 9). This latter toxicity is termed vascular targeting.

BTO-956 [methyl-3,5-diiodo-4-(4′-methoxyphenoxy)benzoate; Fig. 1] was originally developed as a thyroid hormone analogue, but failed to show any physiological activity associated with thyroid hormone metabolism (10). However, in recent studies we demonstrated that BTO-956 inhibits the proliferation of human carcinoma cells *in vitro* and that it has potent growth delay activity in human breast and ovarian carcinoma xenografts in nude mice (11, 12). In addition, we found that the cytotoxicity of BTO-956 toward tumor cells involves mitotic arrest associated with disruption of cellular microtubule assembly that probably arises from binding of the drug to the colchicine site of

Received 1/2/01; revised 5/14/01; accepted 5/15/01.

The costs of publication of this article were defrayed in part by the payment of page charges. This article must therefore be hereby marked *advertisement* in accordance with 18 U.S.C. Section 1734 solely to indicate this fact.

[1] This research was supported by the California Breast Cancer Research Program (Grant 4CB-0032 to K. R. L.) and Large Scale Biology Corporation, Vacaville, CA.

[2] To whom requests for reprints should be addressed, at Department of Radiation Oncology, Duke University Medical Center, Durham, NC 27710-3455. Phone: (919) 684-4711; Fax: (919) 684-8718; E-mail: dewhirst@radonc.duke.edu.

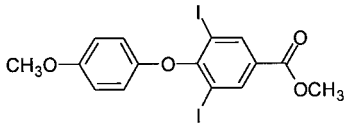

Fig. 1 Structure of BTO-956.

tubulin (12). This finding was unexpected considering the structural similarity of BTO-956 to thyroid hormone, and suggested that it represents a new and novel class of antitumor agent. Because tubulin-binding drugs can have antiangiogenic activity, we hypothesized that BTO-956 could also inhibit angiogenesis. Here we present findings showing that BTO-956 has strong antiproliferative activity toward human microvascular endothelial cells *in vitro* and substantial antiangiogenic activity *in vivo*, as assessed by its effect on rat corneal neovascularization induced by a growth factor (13) and on tumor angiogenesis in a window chamber model of the R3230Ac rat mammary carcinoma (14).

MATERIALS AND METHODS

BTO-956. BTO-956 used in this study is an experimental drug that was synthesized at SRI International by procedures published in the literature (12).

Rat Corneal Neovascularization Assay. Hydron polymer (IFN Sciences, New Brunswick, NJ) was dissolved in absolute ethanol (12% w/v) in a rotator at 37°C overnight and stored at room temperature before pellet making. A stock solution of bFGF[3] (recombinant human bFGF; R&D Systems, Inc., Minneapolis, MN) at a concentration of 200 ng/μl was prepared by dissolving the lyophilized product with sterile PBS containing 0.1% BSA. Aliquots of the stock bFGF solution (5 or 10 μl) were then prepared and stored at −80°C. Sucralfate (sucrose octasulfate aluminum complex; Sigma Chemical Co., St. Louis, MO) stock solution was prepared by suspending Sucralfate in sterile PBS at 100 μg/μl. This solution was stored at 4°C.

Each pellet for the corneal pocket assay contained 50 ng of bFGF and 20 μg of Sucralfate in 3 μl of casting gel, which was constituted as a 50:50 (v/v) mixture of Hydron gel and bFGF-Sucralfate-PBS. The pellets were prepared the day before corneal surgery in a laminar flow hood under sterile conditions. For example, to make 20 pellets, 4 μl of Sucralfate suspension was added to a 5-μl bFGF aliquot. Sterile PBS (21 μl) was then added to this vial and vortexed; 30 μl of Hydron gel was then added, followed by vigorous vortexing for 1 min. This casting gel was promptly pipetted in 3.0-μl drops on a sterile Teflon sheet (Small Parts, Inc., Miami Lakes, FL) in a Petri dish. The Petri dish was placed in a 4°C refrigerator overnight to allow for polymerization. Dried discs of uniform size (~2 mm in diameter) were chosen for use.

Female Fischer 344 rats (n = 16 animals; 8–10 weeks of age; approximate weight, 150 g; Charles River, Raleigh, NC) were used for this study. Animals were kept in temperature-controlled rooms (24°C) on a 12-h light-dark cycle with access to rat chow and tap water *ad libitum*. Following anesthesia with sodium pentobarbital (Abbott Laboratories, North Chicago, IL) given i.p. at 50 mg/kg of body weight, a rat was placed under a dissecting microscope, and a drop of Ophthaine was applied on the cornea of one eye. The eye was proptosed by stretching sutures on the upper and lower eyelids. A small superficial incision was made through the cornea center, and a micropocket was created by separating the lamella of the stroma toward the limbus with a modified iris spatula. The distance between the bottom of the micropocket and the limbus was ~1 mm. A prepared sterile Hydron pellet was rehydrated with a drop of sterile saline and placed into the corneal micropocket. The cornea was covered with gentamicin ophthalmic ointment (Alleran, Inc., Irvine, CA) after surgery. Rats were randomly divided into treated and control groups.

Before administration, BTO-956 was suspended at 150 mg/ml in 0.5% methylcellulose (Sigma) in saline containing 0.1% Tween 80 (Sigma). The drug was administrated by oral gavage at a dose of 500 mg/kg of body weight twice a day for 6 days beginning from the first postoperative day. The controls received vehicle only. Body weights of all animals were monitored and recorded daily. On the 7th postoperative day, animals were anesthetized with sodium pentobarbital (50 mg/kg), and the thoracic aorta was rapidly cannulated in a retrograde fashion with PE 100 tubing. An incision was made in the right auricle for drainage of blood and saline during flushing, and 40–60 ml of saline was injected via the tubing to wash out the blood from the vessels in the upper part of the body until the eyes, ears, and nose became pale. Ten ml of Higgins waterproof India ink (Sanford, Bellwood, IL) were injected via the tubing to visualize corneal vessels. The eyes were enucleated and fixed in 10% neutralized buffered formaldehyde and the corneas were dissected and mounted on slides. Slide-mounted corneal images were taken using a Carl Zeiss MPS intravital microscope (Carl Zeiss, Hanover, MD) with a camera connected to a personal computer equipped with Scion Image software and a frame grabber (Scion Corporation, Frederick, MD).

For the quantitative analysis of corneal neovascularization, various parameters of the corneal images were measured by an investigator who was unaware of the treatment assignment. The shortest distance between the implanted pellet and the limbus was marked as the "mid-line" and was measured. The arc along the limbus for the entire vascularized area was drawn, and the length of the arc was measured (Fig. 2). The circumference of this area (*i.e.*, the arc angle) was calculated by the following equation: Circumference (in clock hours) = Arc length × $360/\pi D/30$, where D is the corneal diameter, obtained by averaging diameters of corneal images at lower magnification from 20 rats. The marked arc was evenly divided into six sections. The perpendicular distances between vessel tips and the limbus at the five intersection points of the arc were measured, and the average vessel length was calculated. The perpendicular distance between the tip of the longest vessel and the limbus (longest vessel length) was also measured. To measure the percentage of vascular area (*i.e.*, the vascular area density), three circles with a diameter of 100 pixels were located between the pellet and the limbus. The central circle was on the mid-line, the

[3] The abbreviations used are: bFGF, basic fibroblast growth factor; HMVEC, human microvascular endothelial cell; VEGF, vascular endothelial growth factor.

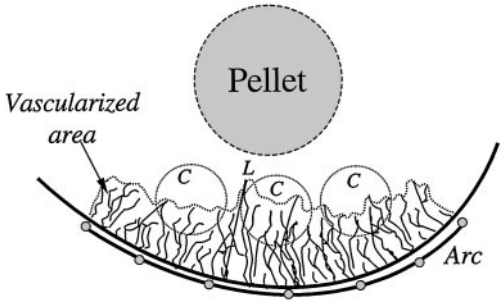

Fig. 2 Method for quantitation of corneal vascularization. The arc (*Arc*) along the limbus for the vascularized area was drawn, and its length was measured for calculation of the circumference of the neovascularized area (*i.e.,* the arc angle). The marked arc was evenly divided into six sections, distances between vessel tips and the limbus at the five intersection points of the arc were measured, and the average vessel length was calculated. The perpendicular distance between the tip of the longest vessel and the limbus (longest vessel length, *L*) was also measured. Three circles (*C*) indicate fields for measuring the vascular area density. The area enclosed by the *dotted line* and the arc was measured and presented as total vascularized area. (See "Materials and Methods" for details).

other two lateral circles were symmetrically placed in each side of the central one in the second and the fifth sections, respectively. The total area (pixel numbers) of each circle (Area-T) and the area for vessels in each circle (total number of black pixels at threshold setting) were measured (Area-V). The vascular area density was defined as the ratio of Area-V to Area-T. An average value from these three circles was obtained for each cornea. Total vascularized corneal area was also measured by marking the perimeter of the vascularized area with image analysis software. Images were calibrated against a stage micrometer image taken at the same magnification and zoom parameters.

Dorsal Skin-Fold Window Chamber Assay. Details of the design and the surgical technique used for the rat dorsal skin-fold window chamber assay have been described elsewhere (14). Briefly, the anatomical midline of the dorsal skin flap of an anesthetized rat was sutured to a pair of C clamps, and the skin-fold was retracted from the body surface by hanging the C clamp on a plastic surgical stage. A 1-cm circle of skin on each side of the skin-fold was surgically removed, leaving two layers of fascia containing a few microvessels. After a pair of window frames were mounted on both sides of the flap, a piece of a R3230Ac rat mammary carcinoma ($\sim$0.5 mm^3) from a donor rat was implanted onto the fascia in the window and the chamber was sealed with glass coverslips. On the 4th postoperative day, all tumor-containing windows were evaluated using an intravital microscope equipped with a video camera. Two investigators observed live images from the camera monitor and crudely scored the viability of the tumor implants in each window chamber, with 1 to 3 points assigned to the categories of size, vascular morphology, and blood flow. Thus, by drawing implant perimeters for images of individual window chambers on a transparency sheet in front of the monitor, implant sizes were compared and scored as follows: 1, small implant, or an implant with visible necrotic areas; 2, medium implant; and 3, large implant. Similarly, vascular morphology was scored as follows: 1, scant few blood vessels, especially around the tumor implant; 2, moderately abundant blood vessels; and 3, abundant blood vessels or newly formed vessels adjacent to the implant. For evaluating blood flow, the following scores were used: 1, less than one-third of the visible blood vessels had active flow around the implant; 2, functioning vessels were observed in more than one-third but less than two-thirds of the total vessels; and 3, more than two-thirds of the vessels were functioning with brisk blood flow. Only those windows with $>$6 points on this scale were included for further study. In many prior studies in untreated animals, we have found that this selection procedure effectively eliminates chamber preparations that fail to grow tumors for various technical reasons.

Tumor-window-bearing animals were randomly divided into treated and control groups, stratified by the window scores. Treatment with BTO-956 was performed from the 5th to the 11th postoperative day at the same doses as those described above for the corneal neovascularization assay. On day 12, the tumor windows were evaluated for the effect of the drug on tumor growth and vascularization. Tumor areas were measured with lower magnification images (objective, $\times$5 or $\times$2.5, depending on tumor size) of whole tumors. Tumor vasculature was evaluated based on four peripheral tumor areas, three to four central tumor areas (depending on tumor size), and four areas in the surrounding granulating tissue, using higher magnification (objective, $\times$20). Measurements were made by an investigator who was unaware of the treatment protocol. Image analysis software, combined with observation of videotaped images showing blood flow, was used to measure the cumulative length of all vessels in focus in each image. The vascular length density was calculated by dividing the total vessel length in a frame by the area of the frame. The diameters of all vessels in each image at high magnification were also measured and averaged. All measurements were calibrated against micrometer images at the same magnification.

Effect of BTO-956 on Proliferation of R3230Ac Rat Mammary Carcinoma and HMVECs. To investigate the effect of BTO-956 on proliferation of R3230Ac cells, cells were first plated at 10^6 cells/100-mm-diameter plastic culture dish in DMEM containing 10% fetal bovine serum (Sigma) and 25 mM HEPES (pH 7.4), and incubated at 37°C in 5% CO_2 for 2 days. Cells were then plated in a 96-well culture plate at 2×10^3 cells/well in 100 μl of DMEM-HEPES-10% fetal bovine serum and incubated at 37°C overnight. Normal HMVECs isolated from dermis were obtained from Clonetics Corporation (Walkersville, MD) and cultured on 100-mm-diameter plastic culture dishes in EGM-2-MV growth medium according to the supplier's instructions. HMVECs were incubated in a 5% CO_2-air atmosphere at 37°C until they were 70–90% confluent, and then were plated in a 96-well culture plate at 5×10^3 cells/well in 100 μl of EGM-2-MV and incubated at 37°C overnight. BTO-956 was added to both cell types over the concentration range 0–10 μM; cells were then incubated at 37°C for 3 days. The effect of BTO-956 on cell proliferation was measured on the 4th day using the nontoxic redox-sensitive dye Alamar Blue in a colorimetric assay.

Statistical Analysis. All data were reported as the mean $\pm$ SE for each group. The statistical significance of

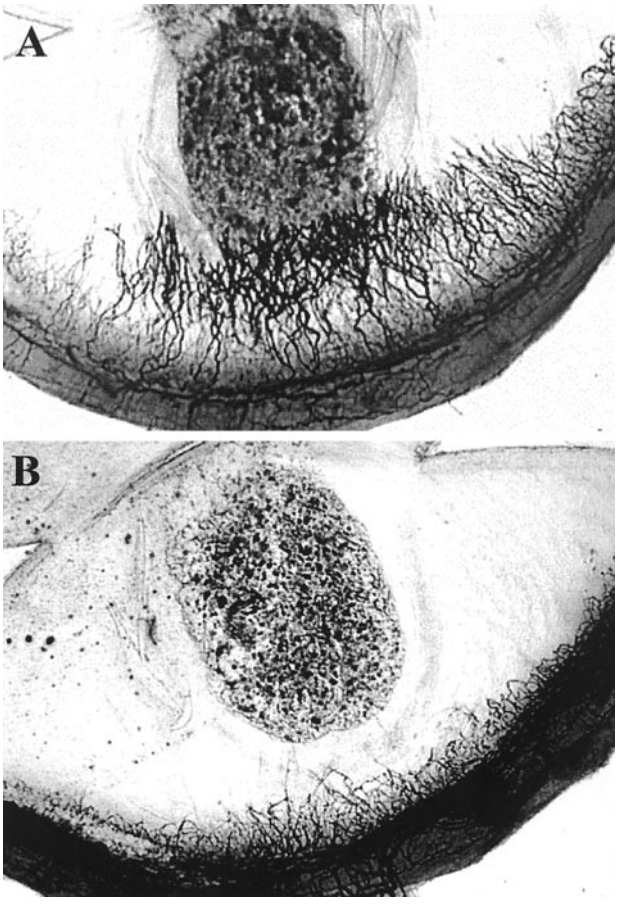

Fig. 3 Typical images of corneal neovascularization induced by bFGF. A polymer pellet containing 50 ng of bFGF was implanted into a surgically created corneal micropocket (the *oval dark area*) in one eye of a Fischer 344 rat. BTO-956 (500 mg/kg) was administered p.o. twice a day during postoperative days 1–6. Control animals received vehicle only. On day 7, the corneal neovasculature was visualized by ink angiography (for details, see "Materials and Methods"). In control animals, abundant new vessels grew from the limbus toward the pellet (*A*), whereas newly formed vessels in the corneas of rats treated with BTO-956 were scarce (*B*).

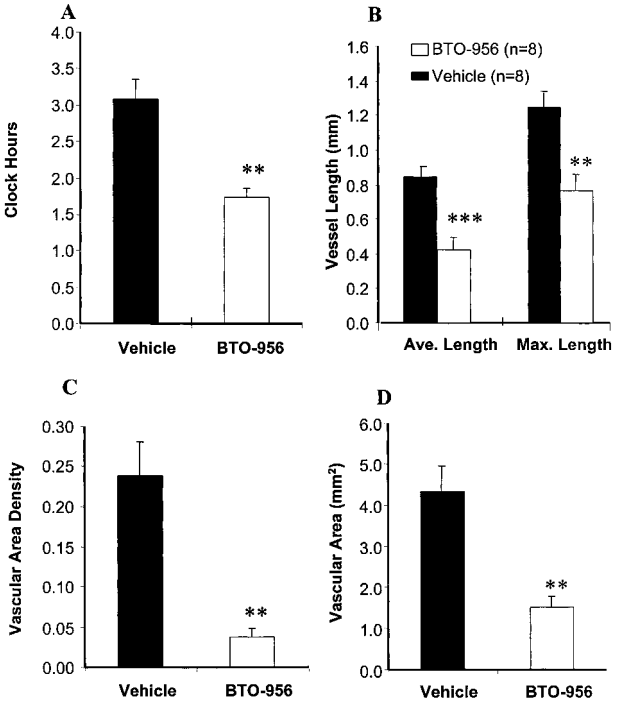

Fig. 4 Quantitative comparison of corneal neovascularization induced by bFGF in Fischer 344 rats. All parameters associated with corneal neovascularization were significantly lower in BTO-956-treated animals (□) compared with controls (■). The circumference values (*Clock Hours*) for corneal neovascularization in treated and control animals were 1.7 ± 0.1 ($n = 8$) and 3.1 ± 0.3 ($n = 8$), respectively (*A*). The average vessel lengths in treated and control animals were 0.4 ± 0.1 mm ($n = 8$) and 0.8 ± 0.1 mm ($n = 8$), respectively. The maximum vessel lengths in treated and control animals were 0.8 ± 0.1 mm ($n = 8$) and 1.2 ± 0.1 mm ($n = 8$), respectively (*B*). The vascular area densities in treated and control animals were 0.04 ± 0.01 ($n = 8$) and 0.24 ± 0.04 ($n = 8$), respectively (*C*). The total vascular areas in treated and control animals were 1.5 ± 0.3 mm^2 ($n = 8$) and 4.3 ± 0.6 mm^2 ($n = 8$), respectively (*D*). *Bars*, SE. **, $P < 0.01$; ***, $P < 0.001$.

differences between treated and control groups was determined using an unpaired *t* test or the Mann-Whitney *U* test. Statistically significant differences were defined as having a $P < 0.05$.

RESULTS

No significant body weight loss or behavioral changes were found for any animals treated with BTO-956 in either study. This result concerning the safety of BTO-956 is consistent with those of previous *in vivo* studies showing that the drug is well tolerated by animals given similar doses administered orally (12).

BTO-956 Inhibits Corneal Angiogenesis. The pellet sizes and the distances between the pellet and the limbus for each group were similar (data not shown). Corneal neovascularization induced by bFGF in BTO-956-treated animals was markedly reduced compared with vehicle-treated control animals (Fig. 3). Quantitative comparison showed that all parameters relevant for measuring the extent of corneal neovascularization were significantly lower in BTO-956-treated compared with control animals. The circumference of neovascularization in treated rat corneas was reduced by 45% compared with controls ($P < 0.01$; Fig. 4*A*). Average and maximum vessel lengths were reduced by 50% ($P < 0.001$) and 38% ($P < 0.01$; Fig. 4*B*), respectively, and the vascular area density and the total vascular area were decreased by 84.5% ($P < 0.01$; Fig. 4*C*) and 65% ($P < 0.01$; Fig. 4*D*), respectively, compared with controls.

BTO-956 Inhibits Tumor Growth and Angiogenesis. Tumors growing in windows of BTO-956-treated animals were much smaller than those in controls (Fig. 5). The treated tumors were also less vascularized, especially in the periphery where angiogenesis is prominent. Specifically, tumor areas were reduced >50% in BTO-956-treated compared with control animals: 23.8 ± 2.5 mm^2 ($n = 8$) for control animals *versus* 10.8 ± 3.4 mm^2 ($n = 9$) for treated animals ($P < 0.05$; Fig. 6*A*). Vascular length density in peripheral tumor areas in BTO-956-treated animals was significantly less than that of the controls: 5.9 ± 0.8 mm/mm^2 ($n = 9$) for treated animals *versus* 7.8 ± 0.6

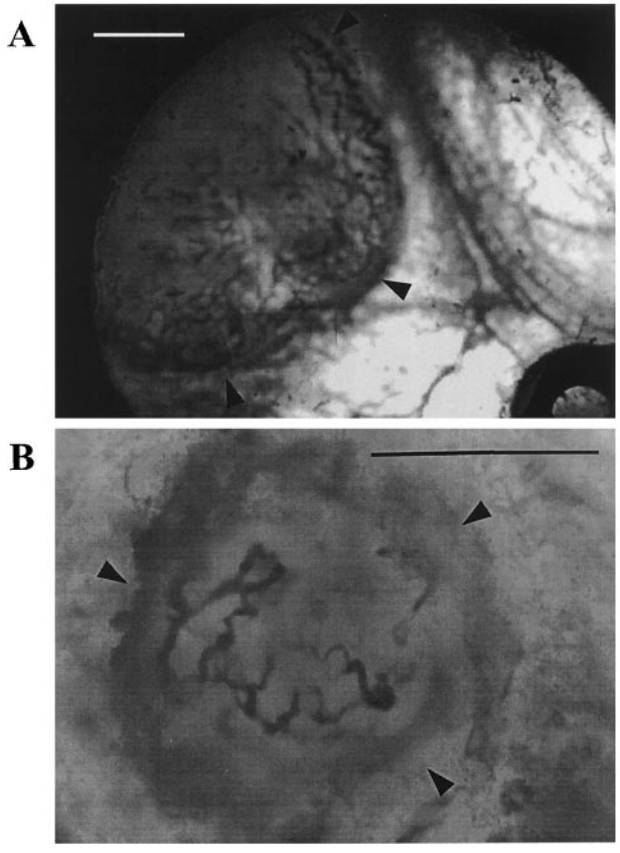

Fig. 5 Inhibition of tumor growth and angiogenesis in the rat dorsal skin-fold window chamber by orally administered BTO-956. R3230Ac rat mammary carcinoma tumors in window chambers were exposed to BTO-956 or vehicle beginning on day 5 postimplantation for a total of 7 days (for details, see "Materials and Methods"). On day 12, images of the window chambers were taken and analyzed. Tumor area was measured at lower magnification (objective, ×2.5 or ×5, depending on the tumor size). Measurements were calibrated against micrometer images at the same magnification. *A*, representative large tumor with abundant vascularization in a control animal (×2.5). *B*, representative tumor in an animal treated with BTO-956, showing a smaller size and less vascularization (×5), compared with the control image. *Arrowheads* indicate tumor margins. *Bars*, 800 μm.

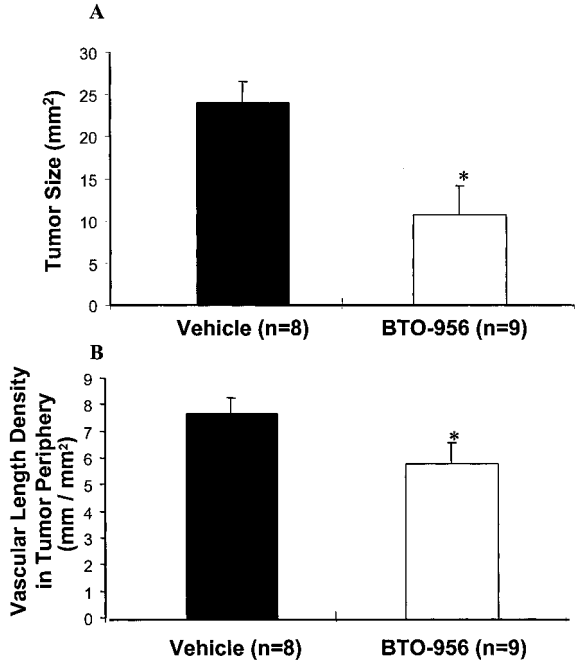

Fig. 6 Quantitative comparison of the effect of BTO-956 on the growth and neovascularization of the R3230Ac rat mammary carcinoma implanted in rat dorsal skin-fold window chambers in Fischer 344 rats. The average sizes of tumors in BTO-956-treated and control animals, as estimated by measurements of two-dimensional areas, were 10.8 ± 3.4 mm^2 (n = 8) and 23.8 ± 2.5 mm^2 (n = 9), respectively (*A*). The vascular length densities in the peripheral tumor zones in treated and control animals were 5.9 ± 0.8 mm/mm^2 (n = 9) and 7.8 ± 0.6 mm/mm^2 (n = 8), respectively (*B*). *Bars*, SE. ∗, $P < 0.05$.

mm/mm^2 (n = 8) for controls ($P < 0.05$; Fig. 6*B*). In contrast, there was no significant difference in the vascular length density between treated and control groups in central tumor areas [3.3 ± 0.8 mm/mm^2 (n = 9) for treated animals *versus* 4.2 ± 0.2 mm/mm^2 (n = 8) for controls] or in surrounding granulating tissue [8.7 ± 1.1 mm/mm^2 (n = 9) for treated animals *versus* 8.7 ± 0.8 mm/mm^2 (n = 8) for controls]. Vascular diameter in the central tumor areas was larger than that in peripheral tumor areas in both groups. However, there were no significant differences in vascular diameter between the two groups in the peripheral tumor areas [32.2 ± 4.5 μm (n = 9) for treated animals *versus* 36.2 ± 5.3 μm (n = 8) for controls], central tumor areas [35.8 ± 9.6 μm (n = 9) for treated animals *versus* 32.0 ± 4.4 μm (n = 8) for controls], or surrounding areas [21.5 ± 3.3 μm (n = 9) for treated animals *versus* 19.2 ± 1.4 μm (n = 8) for controls].

Effect of BTO-956 on Proliferation of R3230Ac Tumor Cells and HMVECs *in Vitro*. Fig. 7 shows that BTO-956 inhibited the *in vitro* proliferation of R3230Ac cells with an IC_{50} (the concentration required to decrease the number of cells by 50% relative to the control) of ~400 nM. Using the same *in vitro* assay, we found that BTO-956 also inhibited the proliferation of HMVECs with an IC_{50} of ~200 nM (Fig. 7). Therefore, consistent with other findings reported for tubulin-binding drugs, BTO-956 can inhibit the proliferation of both tumor and normal microvascular endothelial cells.

DISCUSSION

The major findings of this study are that oral administration of the tubulin-binding drug BTO-956 inhibited (*a*) bFGF-induced rat corneal neovascularization and (*b*) tumor growth and angiogenesis of the R3230Ac rat mammary carcinoma. The antiangiogenic activity of BTO-956 was detectable in the peripheral areas of these implanted tumors, where the most active angiogenesis occurs (15, 16). These effects of BTO-956 are consistent with a growing body of literature suggesting that small-molecule drugs having the ability to disrupt cellular microtubule dynamics can be potent antivascular or antiangiogenic agents (*e.g.*, see Refs. 17, 18). The molecular mechanism of this antiangiogenic effect of BTO-956 is unknown at present. Because BTO-956 can strongly inhibit the proliferation of both

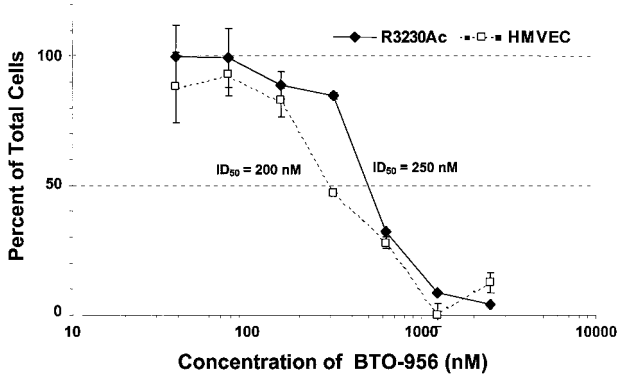

Fig. 7 Effect of BTO-956 on the proliferation of R3230Ac rat mammary carcinoma cells and normal HMVECs *in vitro*. Percentage of total cells (*Percent of Total Cells*) = (number of cells for a treatment concentration − number of cells remaining after the most effective concentration)/(number of untreated or control cells − number of cells remaining after the most effective concentration) × 100. *Bars*, SD.

R3230Ac tumor cells and normal microvascular endothelial cells *in vitro*, it is likely that its ability to inhibit both corneal and tumor angiogenesis involves an effect on endothelial cell proliferation and survival. As reported in our previous study (12), BTO-956 can arrest proliferating tumor cells at a G_2-M checkpoint and cause apoptosis, similar to the effect of other tubulin-binding agents such as colchicine, vinblastine, and paclitaxel. BTO-956 has a structure similar to that of combretastatin A-4 (12), and both of these molecules apparently bind to colchicine sites on β-tubulin. However, whereas combretastatin A-4 has been shown to exert a direct and rapid antivascular effect on tumor microvessels (8, 9), the findings from the corneal neovascularization assay reported here suggest that BTO-956 is more likely to function as an antiangiogenic rather than an antivascular agent. In terms of proangiogenic factors in R3230Ac tumors, we have shown by immunohistochemistry that those tumors express both bFGF and VEGF.[4] We have also found that blockade of VEGF signaling with a soluble VEGF receptor protein blocks neovascularization in these tumors (19) and have shown that SU-5416, a selective inhibitor of VEGF receptor Flk-1, inhibits R3230Ac tumor growth and angiogenesis.[5] However, because BTO-956 is a tubulin-binding drug, presumably its antiangiogenic effect at least partly involves disruption of cellular microtubule networks (12), although it has not been established that β-tubulin is the actual *in vivo* target of the drug. In this connection, recent subcellular fractionation studies have shown that on exposure of R3230Ac cultures to [^{14}C]BTO-956, approximately twice as much label accumulated in the plasma membrane fraction compared with the soluble/cytosolic fraction.[6] Therefore, BTO-956 may have more than one cellular target that could mediate its cytotoxic effect on proliferating cells. Establishing the downstream effectors of the antiproliferative response of vascular endothelial cells to BTO-956 is an important area for further research.

The results from the tumor window chamber assay for the R3230Ac rat mammary carcinoma provide further demonstration that BTO-956 inhibits tumor growth by at least 50%, as assessed by area, compared with controls. Indeed, if the volumes of these tumors were considered, this antitumor effect of BTO-956 would be significantly greater. Other studies have demonstrated that the angiogenic activity in experimental tumors is greatest in peripheral zones (15, 16). Consistent with this conclusion, the results reported here show that the vascular length density in the periphery of the R3230Ac tumor was significantly decreased in the window chambers of BTO-956-treated animals, whereas the vascular length density in central areas of these tumors was unchanged. These findings indicate that the antiangiogenic effect of BTO-956 is most potent in actively angiogenic areas of a tumor.

The *in vitro* study of the effect of BTO-956 on R3230Ac tumor cell proliferation showed cytotoxic or cytostatic activity similar to that described for human breast and ovarian cancer cell lines (11, 12). Therefore, taken with the antiangiogenic effect of BTO-956 detected in the window chamber assay, we suggest that the overall effect of the drug on the growth of the R3230Ac tumor was the result of cytotoxicity toward both angiogenic microvascular endothelial cells and the tumor cells themselves. Finally, as found in our earlier *in vivo* studies of the effect of BTO-956 on tumor growth (12), we observed no serious toxic effects of the drug on tumor-bearing animals, such as weight loss or behavioral abnormalities, even at p.o.-administered doses as high as 500 mg/kg/day given daily for up to 7 days. Further toxicological studies will be necessary to fully evaluate whether BTO-956 has significantly deleterious effects on normal tissues in the rat. Previous pharmacokinetic studies showed that human breast tumor xenografts contained an average of ~9 μg-equivalents of p.o.-administered BTO-956 per g of tumor tissue after oral administration of 0.5 g/kg twice daily for 3 days (12). Therefore, because much of the drug was not bioavailable to these tumor-bearing mice and was excreted, its effect on tumor growth involved only a small fraction of the administered dose. Together with the possibility that BTO-956 may have more than one cellular target mediating both its cytotoxicity and effect on tumor growth, the pharmacokinetic studies provide an explanation for the ability of rodents to tolerate large doses of the drug. These findings indicate that this drug can be administrated p.o. with considerable safety and suggest that it has promise for eventual clinical applications. These applications may require further research concerning formulations to increase the bioavailability of BTO-956 or its derivatives.

In this study, we used vascular length density, as measured in skin-fold window chamber tumors to assess the antiangiogenic activity of this drug during tumor growth. This method is well established as an assay for this end point, as has been reported by others and us (19–23). The difference between this method and simple measurements of microvessel density from histological sections is that the method reflects changes in functional vasculature. In this case, we define functional vasculature as reflecting those vessels that are perfused with red cells. Because the nutrients that are necessary for tumor growth must

[4] Dewhirst *et al.*, unpublished data.
[5] Shan *et al.*, unpublished data.
[6] Laderoute *et al.*, unpublished results.

come from functional vasculature, this method more robustly reflects the physiological effect of an antiangiogenic compound on tumor growth, which is also measured in the same experiment. The process of metastasis also requires tumor cell invasion into functional vasculature. One potential disadvantage of this method is that we are only able to measure vasculature on one surface of the preparation when we use transillumination. It is possible that this measurement does not reflect what is occurring in deeper layers of the tumor. However, this is unlikely because the surface of the tumor represents that region of tumor with most active angiogenesis (15, 16).

Another potential limitation of this method is that mammary tumors are grown in an ectopic site. It is well established that tumor growth and angiogenesis are affected by the site of transplant (24–26). Thus, the degree of angiogenesis inhibition found in this model with BTO-956 might be different from that seen if the tumors were grown in their orthotopic sites. Additional studies would have to be done to determine the magnitude of such an effect, but are outside the scope of the present study.

REFERENCES

1. Folkman, J. Clinical application of research on angiogenesis. Seminars in Medicine of the Beth Israel Hospital, Boston. N. Engl. J. Med., *333:* 1757–1763, 1995.

2. Gasparini, G. The rationale and future potential of angiogenesis inhibitors in neoplasia. Drugs, *58:* 17–38, 1999.

3. Arap, W., Pasqualini, R., and Ruoslahti, E. Chemotherapy targeted to tumor vasculature. Curr. Opin. Oncol., *10:* 560–565, 1998.

4. Presta, M., Rusnati, M., Belleri, M., Morbidelli, L., Ziche, M., and Ribatti, D. Purine analogue 6-methylmercaptopurine riboside inhibits early and late phases of the angiogenesis process. Cancer Res., *59:* 2417–2424, 1999.

5. Ferrante, K., Winnograd, B., and Canetta, R. Promising new developments in cancer chemotherapy. Cancer Chemother. Pharmacol., *43* (Suppl.)*:* S61–S68, 1999.

6. Ludford, R. J. The action of toxic substances upon the division of normal and malignant cells *in vitro* and *in vivo*. Arch. Exp. Zellforsch., *18:* 411–441, 1936.

7. Ludford, R. J. Colchicine in the experimental chemotherapy of cancer. J. Natl. Cancer Inst. (Bethesda), *6:* 89–101, 1945.

8. Dark, G. G., Hill, S. A., Prise, V. E., Tozer, G. M., Pettit, G. R., and Chaplin, D. J. Combretastatin A-4, an agent that displays potent and selective toxicity toward tumor vasculature. Cancer Res., *57:* 1829–1834, 1997.

9. Beauregard, D. A., Thelwall, P. E., Chaplin, D. J., Hill, S. A., Adams, G. E., and Brindle, K. M. Magnetic resonance imaging and spectroscopy of combretastatin A4 prodrug-induced disruption of tumor perfusion and energetic status. Br. J. Cancer, *77:* 1761–1767, 1998.

10. Stasilli, N. R., Kroc, R. L., and Meltzer, R. I. Antigoitrogenic and calorigenic activities of thyroxine analogues in rats. Endocrinology, *64:* 62–82, 1959.

11. Kun, E., Mendeleyev, J., Bauer, P. I., Kirsten, E., Zhen, J., Young, L. T., Vidair, C. A., and Pine, P. Induction of tumor apoptosis by methyl-3,5-diiodo-4-(4′-methoxyphenoxy)benzoate (DIME). Int. J. Oncol., *9* (Suppl.)*:* 829, 1996.

12. Chen, X., Pine, P., Knapp, A. M., Tusé, D., and Laderoute, K. R. Oncocidin A1: a novel tubulin-binding drug with antitumor activity against human breast and ovarian carcinoma xenografts in nude mice. Biochem. Pharmacol., *56:* 623–633, 1998.

13. Polverini, P. J., Bouck, N. P., and Rastinejad, F. Assay and purification of naturally occurring inhibitor of angiogenesis. Methods Enzymol., *198:* 440–450, 1991.

14. Pappenfuss, D., Gross, J. F., Intaglietta, M., and Treese, F. A. A transparent access chamber for the rat dorsal skin fold. Microvasc. Res., *18:* 311–318, 1979.

15. Fukumura, D., Xavier, R., Sugiura, T., Chen, Y., Park, E. C., Lu, N., Selig, M., Nielsen, G., Taksir, T., Jain, R. K., and Seed, B. Tumor induction of VEGF promoter activity in stromal cells. Cell, *94:* 715–725, 1998.

16. Li, C. Y., Shan, S., Huang, Q., Braun, R. D., Lanzen, J., Hu, K., Lin, P., and Dewhirst, M. W. Initial stages of tumor cell-induced angiogenesis: evaluation via skin window chambers in rodent models. J. Natl. Cancer Inst. (Bethesda), *92:* 143–147, 2000.

17. Iyer, S., Chaplin, D. J., Rosenthal, D. S., Boulares, A. H., Li, L. Y., and Smulson, M. E. Induction of apoptosis in proliferating human endothelial cells by the tumor-specific antiangiogenesis agent combretastatin A-4. Cancer Res., *58:* 4510–4514, 1998.

18. Suzuki, M., Okano, A., Tsuji, T., Akiyama, Y., Tsuruo, T., Saito, S., Hori, K., and Sato, Y. Evaluation of antivascular and antimitotic effects of tubulin binding agents in solid tumor therapy. Jpn. J. Cancer Res., *90:* 1387–1395, 1999.

19. Lin, P., Sankar, S., Shan, S., Dewhirst, M. W., Polverini, P. J., Quinn, T. Q., and Peters, K. G., Inhibition of tumor growth by targeting tumor endothelium using a soluble vascular endothelial growth factor. Cell Growth Differ., *9:* 49–58, 1998.

20. Lin, P., Polverini, P., Dewhirst, M., Shan, S., Rao, P. S., and Peters, K. Inhibition of tumor angiogenesis using a soluble receptor establishes a role for Tie2 in pathologic vascular growth. J. Clin. Investig., *100:* 2072–2078, 1997.

21. Jain, R. K., Safabakhsh, N., Sckell, A., Chen, Y., Jiang, P., Benjamin, L., Yuan, F., and Keshet, E. Endothelial cell death, angiogenesis, and microvascular function after castration in an androgen-dependent tumor: role of vascular endothelial growth factor. Proc. Natl. Acad. Sci. USA, *95:* 10820–10825, 1998.

22. Haroon, Z. A., Hettasch, J. M., Lai, T. S., Dewhirst, M. W., and Greenberg, C. S. Tissue transglutaminase is expressed, active, and directly involved in rat dermal wound healing and angiogenesis. FASEB J., *13:* 1787–1795, 1999.

23. Haroon, Z. A., Lai, T. S., Hettasch, J. M., Lindberg, R. A., Dewhirst, M. W., and Greenberg, C. S. Tissue response to tumor invasion and inhibits tumor growth. Lab. Investig., *79:* 1679–1686, 1999.

24. Takahashi, Y., Ellis, L. M., Wilson, M. R., Bucana, C. D., Kitadai, Y., and Fidler, I. J. Progressive upregulation of metastasis-related genes in human colon cancer cells implanted into the cecum of nude mice. Oncol Res., *8:* 163–169, 1996.

25. Pettaway, C. A., Pathak, S., Greene, G., Ramirez, E., Wilson, M. R., Killion, J. J., and Fidler, I. J. Selection of highly metastatic variants of different human prostatic carcinomas using orthotopic implantation in nude mice. Clin. Cancer Res., *2:* 1627–1636, 1996.

26. Fukumura, D., Yuan, F., Monsky, W. L., Chen, Y., and Jain, R. K. Effect of host microenvironment on the microcirculation of human colon adenocarcinoma. Am. J. Pathol., *151:* 679–688, 1997.